Kalpa Publications in Computing

Volume 22, 2025, Pages 524–529

Proceedings of The Sixth International Conference on Civil and Building Engineering Informatics

Energy Consumption Modeling for a Robot Arm in 3D Concrete Printing

Tong Liu[1], Song Du[1], Fei Teng[1] and Yiwei Weng[1*]

[1] The Hong Kong Polytechnic University. Hong Kong SAR.

tong3213.liu@connect.polyu.hk, song.du@connect.polyu.hk, fei0708.teng@connect.polyu.hk, yiwei.weng@polyu.edu.hk

Abstract

The construction sector is a major contributor to global CO2 emissions and energy consumption. 3D concrete printing (3DCP) provides sustainable solutions to tackle the environmental challenges. However, the long-time and continuous operation of robotic arm printers in 3DCP incur critical challenges in energy efficiency. To address these challenges, this study aims to develop an energy consumption (EC) model of a robotic arm in 3DCP. The proposed EC model has desirable agreement compared to the experimental result, achieving an accuracy 99.51%. The impact of the proposed EC model is evaluated by printing a pre-designed path with various positions. Results reveal that the EC reduction can achieve up to 53.72% with varying positions. The findings reveal that the proposed EC model has the potential to reduce the EC for energy efficiency in 3DCP.

1 Introduction

The construction sector is a main contributor to global carbon emissions and energy consumption due to the huge amount of cement production (Li et al., 2024). 3D concrete printing (3DCP) provides the potential to address these challenges with enhanced productivity and sustainability (Mechtcherine et al., 2018). Previous research has demonstrated that 3DCP outperforms precast concrete by reducing 25.4% the overall cost, 85.9% in CO_2 emissions, and 87.1% in energy consumption concerning the production of a prefabricated bathroom unit (Weng et al., 2020). However, 3DCP typically exhibits a higher electricity consumption than conventional construction since a long operation of the robotic arm is required for large-scale printing (Zhang et al., 2018). It is pressingly needed to enhance the energy efficiency of robotic operation during printing.

Kajzr et al., (2024) investigated the energy consumption (EC) of a robotic arm in 3DCP in a simulated environment. The results demonstrate that the motion characteristics of robotic arms and

* Corresponding authors.

their operational scenarios significantly influence energy consumption, presenting challenges for accurate energy modeling. The EC behavior of a robotic arm is determined by the joint configurations, motion trajectories, and tasks (Wang et al., 2018). Most of the existing EC optimization methods mainly focus on specific applications such as welding (Zhou et al., 2022), polishing (Cao et al., 2020), and other assembly processes (Soori et al., 2023). For instance, Pellicciari et al., (2013) and Feng et al., (2021) proposed methods to optimize robotic trajectories for energy-saving in pick-and-place tasks. The results show that a 10% reduction of EC reduction can be achieved based on flexible joint configurations (Feng et al., 2021). Liu et al., (2018) investigated the correlation between robot speed and EC, identifying an optimal speed range for energy minimization. Gadaleta et al., (2021) conducted extensive experiments on industrial robots, revealing an energy-saving potential exceeding 50%.

However, few studies have been conducted with respect to the application of the EC model in 3DCP. 3DCP typically exhibits unique characteristics compared to the processes abovementioned, including 1) constrained joint configurations due to a vertically fixed concrete extruder, 2) high gravitation and fractional force, and 3) the requirement of a continuous toolpath. To fill the above research gaps, the first step is to construct the EC model, taking 3DCP characteristics into account. In this study, firstly, an EC model compatible with 3DCP is proposed. The EC model is established by determining a parameter set of a robotic arm. The effect of printing positions on the EC behavior of the robotic arm is evaluated using a pre-designed printing path.

2 Method

The movement of a robot is powered by joint torque. Joint torques are associated with the robot's dynamic parameters, including mass, the center of mass, inertia tensor, and frictional joint torque. The robot dynamic model establishes the relationship between joint torque and joint configuration, expressed by:

$$\tau = M(q)\ddot{q} + C(q,\dot{q})\dot{q} + G(q) + \tau_f(q) \tag{1}$$

where τ represents the joint torque vector, q, $\dot{q}$, and $\ddot{q}$ are joint position vector, joint velocity vector, and joint acceleration vector, respectively. $M(q)$ is the positive definite inertia matrix, $C(q,\dot{q})$ is the Coriolis-Centrifugal matrix, $G(q)$ is the torque vector induced by gravity. $\tau_f(q)$ is the frictional vector. In this study, the friction vector can be formulated as (Paes et al., 2014):

$$\tau_f(\dot{q}) = f_v\dot{q} + f_c sign(\dot{q}) \tag{2}$$

where the f_v and f_c represent viscous and Coulomb friction coefficients, respectively.

For each link, a set of dynamic parameters needs to be determined, including the mass (m_i), center of mass ($\boldsymbol{C}_{m,i}$), the inertia tensor ($\boldsymbol{I}_{m,i}$), as well as vicious (f_{vi}) and Coulomb friction items (f_{ci}). The dynamic parameter vector (π_i) of link typically contains parameters related to the mass, center of mass, and inertia:

$$\pi_i = [\, m_i, \boldsymbol{C}_{m,i},\ \boldsymbol{I}_{m,i},\ f_c,\ f_v] \tag{3}$$

and a dynamic parameter set ($\boldsymbol{\Pi}$) to represent the collection of robot dynamic parameters:

$$\boldsymbol{\Pi} = [\pi_1, \pi_2, \dots, \pi_6]^T \tag{4}$$

where $\boldsymbol{\Pi}$ defines the used to create the robot links object. The robot object can be created based on the determined parameter set $\boldsymbol{\Pi}$. Afterward the modeled joint torque τ^{mod} can be calculated by the recursive Newton-Euler method *rne*, given joint position q, velocity $\dot{q}$, and acceleration $\ddot{q}$ (Chignoli et al., 2023). This operation can be represented by:

$$\tau = rne(q,\dot{q},\ddot{q}) \tag{5}$$

the robot real-time power $P(t)$ satisfies:

$$P(t) = \tau(t)q(t) \tag{6}$$

during a time period of robotic motion T, the total EC can be calculated with Eq. (6):

$$E = \int_T P(t)dt \tag{7}$$

Rapid is a programming language designed to control robotic systems. In the motion of a robot, the joint data can be collected via the function of *GetJointData* in Rapid and sent to the computer. The collected data, including joint torque τ^{col} and joint configuration $(q, \dot{q}, \ddot{q})^{col}$, can be used to calculate the collected power $P^{exp}(t)$ and total EC E^{exp} by Eqs. (6) and (7) from experiment, respectively. It should be noted that *GetJointData* cannot provide the data of joint acceleration, and therefore, the collected joint acceleration $(\ddot{q}_{col})$ is calculated numerically through a central finite difference method (Teixeira et al., 2023). The modeled power $P^{mod}(t)$ and EC E^{mod} from the experiment is calculated by Eqs. (5)~(7) using the collected joint configurations $(q, \dot{q}, \ddot{q})^{col}$.

The dynamic parameter set **Π** can be determined by minimizing the variance between the collected real-time power $P^{col}(t)$ and modeled power $P^{mod}(t)$, which are discrete data. The total number of collected discrete data is labeled as *N*, P_n^{col}, and P_n^{mod}, utilized to represent *n*-th collected and modeled instantaneous power. To determine the dynamic parameter set, an objective function is defined as below:

$$C = \sqrt{\frac{1}{N}\sum_{n=1}^{N}\left(P_n^{exp} - P_n^{mod}\right)} \tag{8}$$

where the objective function *C* indicates the difference between the collected and modeled power. Once the dynamic parameters set **Π** is determined, the objective function *C* reaches its minimum.

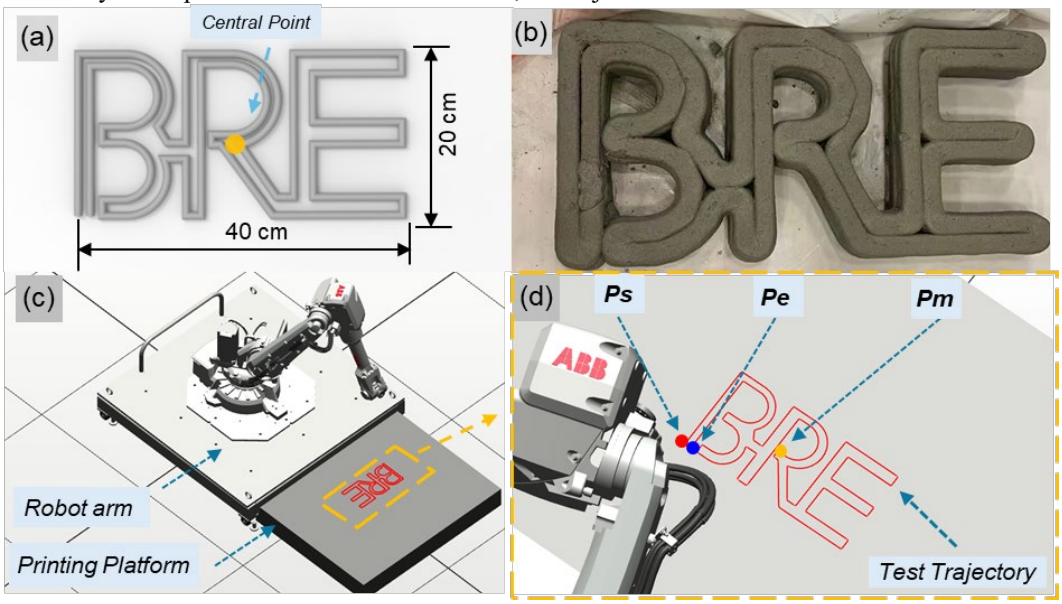

Figure 1: Motion trajectory illustration: (a) dimensions of the printing path; (b) printed specimens; (c) printing setup and area; (d) a continuous robot trajectory for printing.

In this study, the test trajectory is pre-defined for dynamic parameter determination. As shown in Figure 1 (a), a pre-designed printing path is adopted for experiment, and the position is represented by a central reference point. Figure 1 (b) illustrates the printed concrete structures along the pre-designed path. Figure 1 (c) shows the setup of the printing task, and Figure 1 (d) presents the start point (*Ps*), middle point (*Pm*), and end point (*Pe*) in the trajectory for power comparison. The real-time power data (P_i^{col}) will be collected during the robotic operation. The dynamic parameter set of the robot arm will be determined to construct the EC model by minimizing the defined objection function *C* in Eq. (8).

3 Results and Discussion

3.1 Comparison between Modeled and Collected Test Trajectory

In this work, **Π** and C are regarded as independent and dependent variables, respectively, and the function of *fminunc* in Matlab-2024 is applied to optimize C and determine the parameter set **Π**. Then, the real-time power and the EC behavior during robot motion can be determined in theoretical models.

Figure 2 (a) shows the comparison between the theoretical and experimental instantaneous power-time curves. The local maximum can be detected when the end effector moves at the *Pm*. At least five experiments were conducted for the test trajectories. The EC can be calculated by employing Eq. (6), and experimental and simulation results can be seen in Figure 2 (b). The accuracy of EC prediction is 99.51%, indicating that the proposed EC model is reliable in predicting the EC values during the motion of the robot arm.

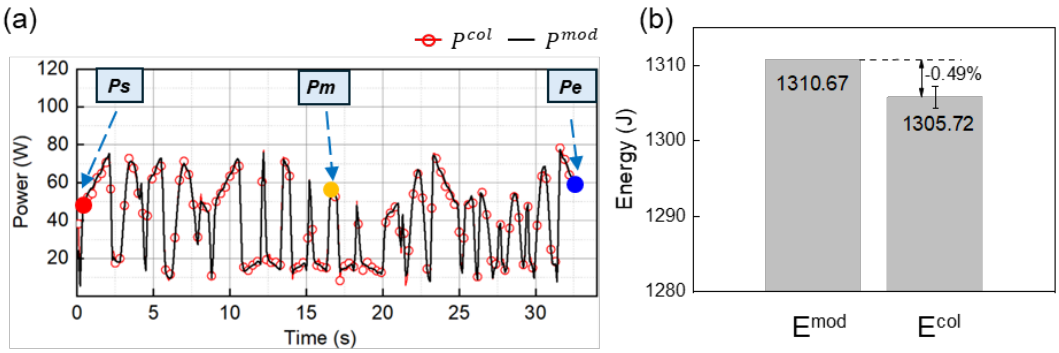

Figure 2: Results to determine model parameters. (a) comparison between the theoretical and experimental results of real-time power P^{mod} and P^{col}; (b) comparison of the theoretical and experimental results for a printed BRE path.

3.2 Impact of Position on EC Behavior

As stated above, for a given trajectory, the EC value can be calculated via the proposed EC models with the determined parameter set **Π**. Then, the effect of printing positions on EC was evaluated. Five different positions within the working area of the robot were used in this study. Figure 3 (a) shows the printing setup and five different positions. The coordinate data of these positions are referenced to the base frame and are listed in Table 1. Figure 3 (b) shows the printing paths with different positions *P1~P5*, which are located at the four corners and the central location of the working area.

Points	Position (mm)
*P*1	(1100, 400, 0)
*P*2	(1100, -400, 0)
*P*3	(1400, -400, 0)
*P*4	(1400, 400, 0)
*P*5	(1250, 0, 0)

Table 1: Coordinates of different positions.

During the robot motion in the virtual environment, the collected joint configuration $(q, \dot{q}, \ddot{q})^{col}$ can be obtained for EC calculations. Figure 4 presents the simulated result of EC values for positions *P*1~*P*5. The results show that the EC value in position *P4* is the highest, 2,497.6J, comparable to the

EC value in position *P3*. The EC value in position *P2* is the lowest, 1,151.2J, comparable to the EC value in positions *P1* and *P5*, 1,185.4J and 1,237.8J, respectively. Results reveal that the EC value can be reduced by 53.72% between the maximum (*P4*) and minimum (*P2*) values among different positions. This is mainly attributed to the different robot configurations during the printing. In practical applications, printing positions can be regarded as an optimal factor in the EC model for printing path-planning to realize energy efficiency and lower carbon emissions in the 3DCP process.

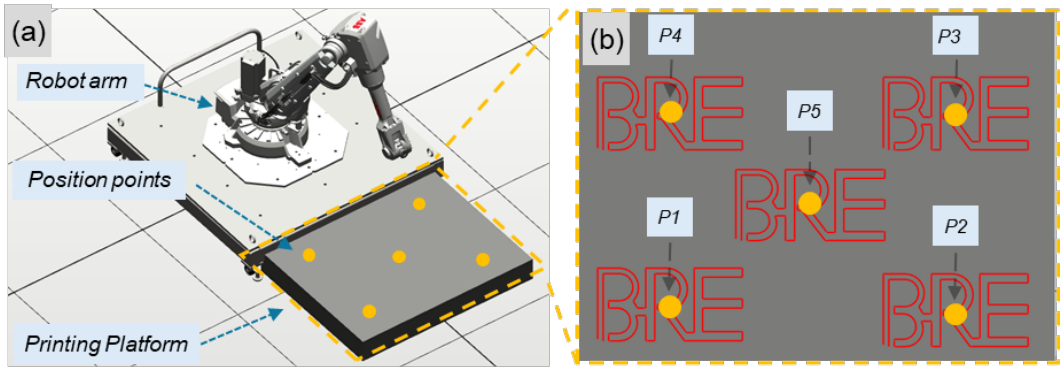

Figure 3: Diagram for various positions: (a) printing setup and printing platform; (b) pre-designed path at different printing positions of P1~P5 on the printing platform.

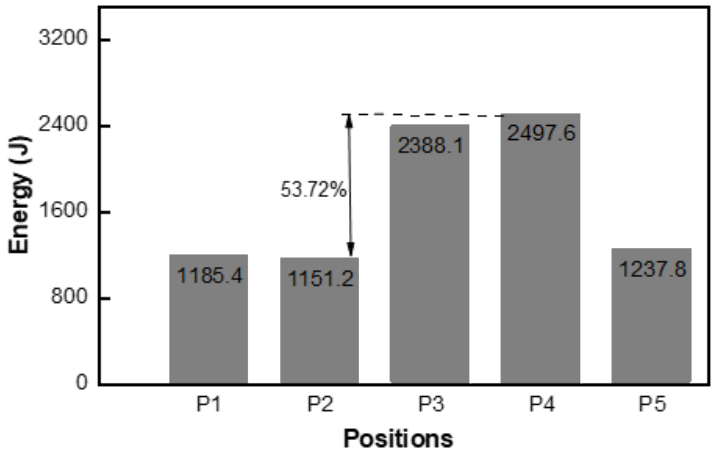

Figure 4: Simulated EC at different printing positions.

4 Conclusion

This study integrates the construction characteristics of 3D concrete printing (3DCP) with the dynamic parameters of robotic arms to develop an energy consumption model tailored for 3DCP operations. The proposed model provides energy consumption analyses for both printing positions and printing paths in 3DCP, thereby facilitating the achievement of low-carbon construction. The EC model is constructed by the determination of the dynamic parameter set Π. Then, the effect of the printing positions on EC is explored in 3DCP. Results show that a 99.51% accuracy of the modeled EC behavior can be achieved compared to that of the experimental results. The EC can be reduced by 53.72% with the optimization of the printing position for the pre-designed path. This proposed EC

model for 3DCP provides a novel design method for researchers and designers to enhance energy efficiency in 3DCP processes.

5 Acknowledgments

The author would like to gratefully acknowledge the Project No.52308284 supported by National Natural Science Foundation of China and the Hong Kong Polytechnic University.

6 References

Cao, H., Zhou, J., Jiang, P., Hon, K. K. B., Yi, H., & Dong, C. (2020). An integrated processing energy modeling and optimization of automated robotic polishing system. *Robotics and Computer-Integrated Manufacturing*, 65, 101973.

Chignoli, M., Adrian, N., Kim, S., & Wensing, P. M. (2023). Recursive Rigid-Body Dynamics Algorithms for Systems with Kinematic Loops. arXiv preprint arXiv:2311.13732.

Feng, Y., Ji, Z., Gao, Y., Zheng, H., & Tan, J. (2021). An energy-saving optimization method for cyclic pick-and-place tasks based on flexible joint configurations. *Robotics and Computer-Integrated Manufacturing*, 67, 102037.

Gadaleta, M., Berselli, G., Pellicciari, M., & Grassia, F. (2021). Extensive experimental investigation for the optimization of the energy consumption of a high payload industrial robot with open research dataset. *Robotics and Computer-Integrated Manufacturing*, 68, 102046.

Kajzr, D., Myslivec, T., & Černohorský, J. (2024). Modelling, Analysis and Comparison of Robot Energy Consumption for Three-Dimensional Concrete Printing Technology. *Robotics*, 13(5), 78.

Li, K., Zou, Z., Zhang, Y., & Shuai, C. (2024). Assessing the spatial-temporal environmental efficiency of global construction sector. *Science of The Total Environment*, 951, 175604.

Liu, A., Liu, H., Yao, B., Xu, W., & Yang, M. (2018). Energy consumption modeling of industrial robot based on simulated power data and parameter identification. *Advances in Mechanical Engineering*, 10(5), 1687814018773852.

Mechtcherine, V., Grafe, J., Nerella, V. N., Spaniol, E., Hertel, M., & Füssel, U. (2018). 3D-printed steel reinforcement for digital concrete construction–Manufacture, mechanical properties and bond behaviour. *Construction and Building Materials*, 179, 125-137.

Pellicciari, M., Berselli, G., Leali, F., & Vergnano, A. (2013). A method for reducing the energy consumption of pick-and-place industrial robots. *Mechatronics*, 23(3), 326-334.

Teixeira, F., Sarris, C., Zhang, Y., Na, D.-Y., Berenger, J.-P., Su, Y., Okoniewski, M., Chew, W., Backman, V., & Simpson, J. J. (2023). Finite-difference time-domain methods. *Nature Reviews Methods Primers*, 3(1), 75.

Wang, L., Mohammed, A., Wang, X. V., & Schmidt, B. (2018). Energy-efficient robot applications towards sustainable manufacturing. *International Journal of Computer Integrated Manufacturing*, 31(8), 692-700.

Weng, Y., Li, M., Ruan, S., Wong, T. N., Tan, M. J., Yeong, K. L. O., & Qian, S. (2020). Comparative economic, environmental and productivity assessment of a concrete bathroom unit fabricated through 3D printing and a precast approach. *Journal of Cleaner Production*, 261, 121245.

Zhang, X., Li, M., Lim, J. H., Weng, Y., Tay, Y. W. D., Pham, H., & Pham, Q.-C. (2018). Large-scale 3D printing by a team of mobile robots. *Automation in Construction*, 95, 98-106.